Progress in Earth
and Planetary Science
a SpringerOpen Journal

REVIEW

Open Access

CrossMark

Sea surface temperature proxies (alkenones, foraminiferal Mg/Ca, and planktonic foraminiferal assemblage) and their implications in the Okinawa Trough

Ryoung Ah Kim, Kyung Eun Lee[*] and Si Woong Bae

Abstract

We reviewed three sea surface temperature (SST) proxies in the Okinawa Trough (OT): alkenones, planktonic foraminiferal Mg/Ca, and planktonic foraminiferal assemblages. The seasonal and vertical distribution patterns of each proxy-related organism in the water column were reviewed to confirm the applicability of each proxy. In addition, current SSTs (Japan Oceanographic Data Center dataset from 1906 to 2003) were compared with core-top sediment temperatures reconstructed using the proxies. Temperatures calculated using the alkenone unsaturation index represent annual mean SSTs, and temperatures calculated using Mg/Ca of *Globigerinoides ruber* capture summer to autumn (June–November) SSTs. Core-top August SSTs calculated from planktonic foraminiferal assemblages corresponded well with the observed SSTs, but core-top February temperatures were ~3.6 °C warmer than the observed SSTs. SST proxy estimates from marine sediments dating back to the late Holocene (0–3 cal ky BP) and the last glacial maximum (18–21 cal ky BP) were compared. Comparisons between proxy SST estimates show that foraminiferal assemblage-based August SSTs were the warmest. Alkenone-based temperature estimates were lower than Mg/Ca-based temperature estimates, probably because the alkenone-based temperature represents the annual mean temperature, whereas the Mg/Ca-based temperature represents the summer–autumn mean temperature. February assemblage SSTs seem to be greatly affected by the statistical technique and/or database used. These results suggest that seasonality should be considered in past SST reconstruction using alkenone and Mg/Ca in the OT. The planktonic foraminiferal assemblage technique does not appear to be promising with respect to accurately reconstructing past SSTs (especially winter) in the OT. Habitat depth may not be an issue because both alkenone producers and *G. ruber* live at the upper surface mixed layer in the area.

Glacial–interglacial changes in the surface hydrography of the OT reconstructed based on the SST and salinity proxies were also reviewed here. The surface hydrography of the OT has been influenced by changes in the Kuroshio Current and the East Asian monsoon system during the late Quaternary. Comparisons of the hydrography records from the OT with records of stalagmites in China, the Tropical Pacific, and the North Atlantic show that there is a teleconnection between them.

Keywords: Sea surface temperature, Okinawa Trough, Alkenone, Planktonic foraminiferal Mg/Ca ratio, Planktonic foraminiferal assemblages

* Correspondence: kyung@kmou.ac.kr
Ocean Science and Technology School, Korea Maritime and Ocean University, Busan 606-791, South Korea

Springer

Kim *et al. Progress in Earth and Planetary Science* (2015) 2:43

Page 2 of 16

Review

Introduction

The Okinawa Trough (OT) is a back-arc basin located behind the Ryukyu arc system in the northwestern Pacific. Surface hydrographic changes in the OT have been reconstructed based on various proxies. Past sea surface temperatures (SSTs) in the OT have been reconstructed from various proxies, including alkenone, planktonic foraminiferal Mg/Ca, planktonic foraminiferal assemblages, and glycerol dibiphytanyl glycerol tetraether (GDGT) (Jian et al. 2000; Li et al. 2001; Ujiié et al. 2003; Ijiri et al. 2005; Sun et al. 2005; Lin et al. 2006; Zhou et al. 2007; Chang et al. 2008; Yu et al. 2009; Chen et al. 2010; Kubota et al. 2010; Nakanishi et al. 2012a). Past sea surface salinities (SSSs) have been reconstructed based on oxygen isotope ratios of foraminifera and SST proxies (Ujiié et al. 2001, 2003; Ijiri et al. 2005; Sun et al. 2005; Yu et al. 2009; Kubota et al. 2010). Many previous studies have shown that the surface hydrography of the OT has been influenced by changes in the Kuroshio Current (KC) (Jian et al. 2000; Lin et al. 2006) and the East Asian monsoon system (Li et al. 2001; Sun et al. 2005; Zhou et al. 2007; Chang et al. 2008; Chen et al. 2010; Kubota et al. 2010) during the late Quaternary. These suggest that changes in the main axis and volume transport of the KC and the intensity of the East Asian summer monsoon affected the surface changes in the OT.

This paper reviews SST reconstruction techniques in the OT. In addition, glacial–interglacial changes in the surface hydrography of the OT reconstructed based on the SST and SSS proxies are reviewed, as are their implications for paleoclimate changes. As the reconstruction of past SSTs from alkenone, Mg/Ca, and GDGT is based on the information recorded in marine organisms such as coccolithophores, foraminifera, and *Crenarchaeota*, knowledge on the habitat depth and seasonal abundance of these organisms is relevant. It is essential to accurately determine what depth and season are represented by the temperatures estimated using these proxies. Some previous studies have suggested that the alkenone-based temperature might represent the annual mean SST (Yu et al. 2009). However, others have suggested that the alkenone-based temperature represents spring or spring to summer SSTs in the OT (Ijiri et al. 2005; Zhou et al. 2007; Nakanishi et al. 2012a). The *Globigerinoides ruber* Mg/Ca ratio temperature is thought to represent summer or warm season SSTs. GDGT proxy has not been extensively studied in the OT, and the representative depth of GDGT is unclear in this region (Nakanishi et al. 2012a). Thus, there is no consensus on what each proxy represents, and no comparative assessment has yet been published regarding these proxies in the OT.
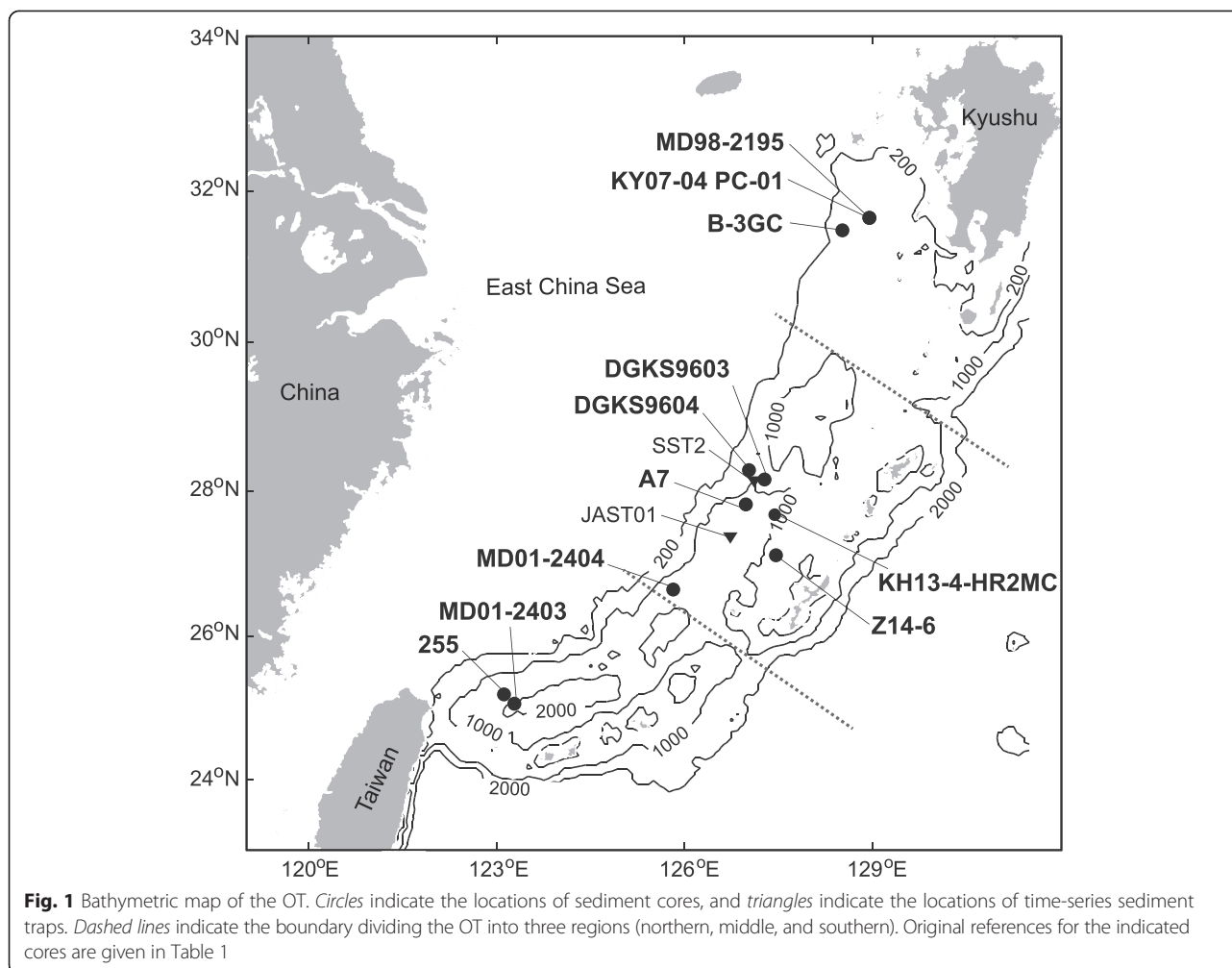
In this review, we compare three temperature proxies for reconstructing SSTs in the OT: alkenones, Mg/Ca, and planktonic foraminiferal assemblages. As there have been few studies regarding GDGT in the OT, we focus our discussion on only the abovementioned proxies. In Section 3, we review the seasonal and vertical distribution patterns of each proxy-related producer in the water column to examine what the proxy temperatures represent. In addition, the proxy temperature estimates from core-top sediments are compared with observed SSTs to confirm that proxy temperatures reconstructed from marine sediments can represent the current SST in the OT. In Section 4, we compare SST proxy data for the late Holocene (0–3 cal ky BP) and the last glacial maximum (LGM, 18–21 cal ky BP). In Section 5, we review glacial–interglacial changes in the surface hydrography of the OT and their paleoclimatological implications.

Compiled sediment cores

The OT is located in the East China Sea at a water depth range of 1000–2000 m (Fig. 1). As shown in Fig. 2, the sediment cores that were recovered from the OT are mainly composed of homogeneous clay, silty clay, silt, and clayey silt (Jian et al. 2000; Li et al. 2001; Ijiri et al. 2005; Sun et al. 2005; Zhou et al. 2007; Kao et al. 2008; Yu et al. 2009; Kubota et al. 2010), except for core MD01-2404, which is composed of nearly homogeneous nannofossil ooze or diatom-bearing nannofossil ooze (Chang et al. 2009). Ash layers, including the Kikai-Akahoya (K-Ah) and the Aira-Tanzawa (AT), were found in cores DGKS9603 and MD98-2195. The K-Ah and AT tephra are likely related to eruptions of the Kikai volcano (7.3 cal ky BP) and the Aira volcano (26–29 cal ky BP), respectively (Machida 2002). There are some coarse-grained materials in cores MD01-2404 (pumice, volcanic glass), A7 (small turbidites), and MD98-2195 (sandy layer). ^{14}C dating results at the upper and lower limits of these coarse layers suggest that sedimentation was largely uninterrupted in these three cores (Fig. 2) (Ijiri et al. 2005; Sun et al. 2005).

Age models for the cores were mainly derived from radiocarbon dating of planktonic foraminifera (Table 1). The version of the calibration program CALIB used in each study is listed in Table 1. CALIB versions 4, 5, and 6 cover the periods of 0–24, 0–26, and 0–50 cal ky BP, respectively. The reservoir age for most of the cores was considered to be 400 y. In core A7, however, a reservoir age of 700 y was used because the converted calendar ages were in good agreement with the K-Ah tephra age (Sun et al. 2005). The ages in core Z14-6 were determined using the correlation between the cores' oxygen isotope curve and the δ^{18}O stack curve (Zhou et al. 2007). Most of the cores have numerous radiocarbon dates, showing sequential age. Age reversals between

Kim *et al. Progress in Earth and Planetary Science* (2015) 2:43

Page 3 of 16

Fig. 1 Bathymetric map of the OT. *Circles* indicate the locations of sediment cores, and *triangles* indicate the locations of time-series sediment traps. *Dashed lines* indicate the boundary dividing the OT into three regions (northern, middle, and southern). Original references for the indicated cores are given in Table 1

adjacent ^{14}C dates were infrequently found, except in core 255 (Fig. 2). Because of the nonsequential age, the part of core 255 that is older than 10 cal ky BP was not used (Jian et al. 2000). Only two age reversals were found among the cores in cores DGKS9604 and MD01-2403.

Sedimentation rates in the northern and southern parts of the OT appear to be higher than those in the central region (Fig. 3, Table 1). During the late Holocene, the sedimentation rates in the northern and southern regions were higher than 50 cm/ky, except in core B-3GC. The sedimentation rates varied within 5–50 cm/ky in the middle OT. During the LGM, sedimentation rates were either similar to or twice as high as those during the late Holocene (Table 1). Overall, sedimentation rates in the OT are high. However, we cannot completely ignore the effect of bioturbation, because the averaged bioturbation depth is 9.8 ± 4.5 cm over the global ocean (Boudreau 1994) and the sampling interval of cores in the OT is in the range of 2–10 cm. However, proxy records are still considered to be significant despite being smoothed by bioturbation.

SST proxies in the OT
Alkenones
The C$_{37}$ alkenone is known to be produced mainly by the haptophyte microalgae *Emiliania huxleyi*. Alkenones can be used to reconstruct SSTs because the degree of unsaturation of alkenones changes with seawater temperature (Brassell et al. 1986). The alkenone unsaturation index U$^{K'}_{37}$ can be calculated as
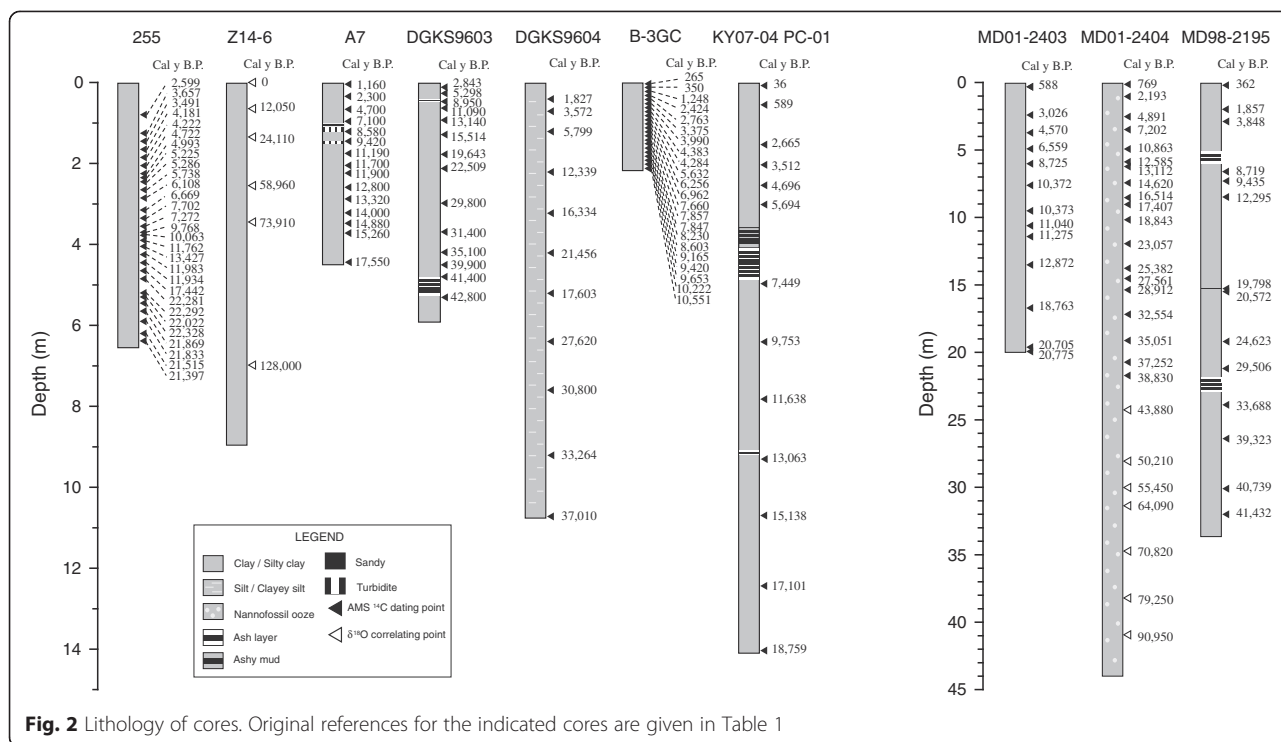
$$U^{K'}_{37} = [C_{37:2}]/([C_{37:2}] + [C_{37:3}]). \tag{1}$$

U$^{K'}_{37}$ is converted to the alkenone-based temperature using one of two calibration equations by Prahl et al. (1988) and Müller et al. (1998), given respectively as

$$T = (U^{K'}_{37} - 0.039)/0.034 \tag{2}$$

$$T = (U^{K'}_{37} - 0.044)/0.033. \tag{3}$$

The Prahl et al. (1988) Eq. (2) stems from an experimental culture of *E. huxleyi*, which is an alkenone producer. The Müller et al. (1998) Eq. (3) is based on a

Kim *et al. Progress in Earth and Planetary Science* (2015) 2:43

Page 4 of 16

Fig. 2 Lithology of cores. Original references for the indicated cores are given in Table 1

comparison between the core-top $U^{K'}_{37}$ and annual mean sea surface (0 m water depth) temperatures. These equations were used in previous studies to reconstruct paleotemperatures in the OT (Table 1) (Ijiri et al. 2005; Zhou et al. 2007; Yu et al. 2009; Nakanishi et al. 2012a).

Habitat depth of alkenone producers

Although paleo-SSTs can be reconstructed using the alkenone unsaturation index (Brassell et al. 1986), alkenone-based temperatures do not always accurately represent the SST, because of ambiguities concerning the habitat depth of alkenone-producing species (Ohkouchi et al. 1999; Lee and Schneider 2005). According to a study that compared observed water column temperatures with alkenone-based temperatures calculated from surface sediments of the central Pacific Ocean, alkenone-based temperatures in the mid-latitudes are consistent with thermocline temperatures (Ohkouchi et al. 1999). Another study also suggested that alkenone-based temperatures represent thermocline temperatures because alkenone concentrations were high at the subsurface in the water column of the central Pacific Ocean (Lee and Schneider 2005). Nakanishi et al. (2012b) investigated the vertical distribution of the alkenone concentration in the OT. They showed that the alkenone concentration is 100–200 ng/L at depths of 0–25 m, whereas it is almost 0 ng/L at depths below 100 m. Moreover, alkenone-based temperatures reconstructed from suspended particulate organic matter were consistent with in situ shallow (above

100 m) water temperatures (Nakanishi et al. 2012b). Thus, Nakanishi et al. (2012b) suggested that alkenone-based temperatures derived from alkenones preserved in sediments can be used to reconstruct SSTs in the OT. However, there may be changes in habitat depth depending on ages.

Seasonality of alkenone producer

Ternois et al. (1996) suggested that seasonal variability in alkenone production should be considered if alkenones are used as a proxy to reconstruct the temperature. Some authors have suggested that alkenone-based temperatures represent annual mean SSTs in the OT (Yu et al. 2009). However, others have argued that alkenone-based temperatures may represent spring to summer SSTs in the OT (Ijiri et al. 2005; Zhou et al. 2007). Tanaka (2003) investigated coccolith fluxes in time-series sediment traps installed in the OT from March 1993 until February 1994 (at station SST2, Fig. 1). In sediment traps suspended close to the sea surface, the relative abundance of *E. huxleyi* was approximately 60 % of the total coccolith flora during spring and summer but fell to less than 30 % for the remaining period. However, in deep-water sediment traps (installed 50 m above the seafloor), *E. huxleyi* fluxes remained constant and constituted approximately 40 % of the total coccolith flora in all seasons. Given this constant flux observed by Tanaka (2003) in deeper waters, alkenone-based temperatures reconstructed from sediments may represent the annual
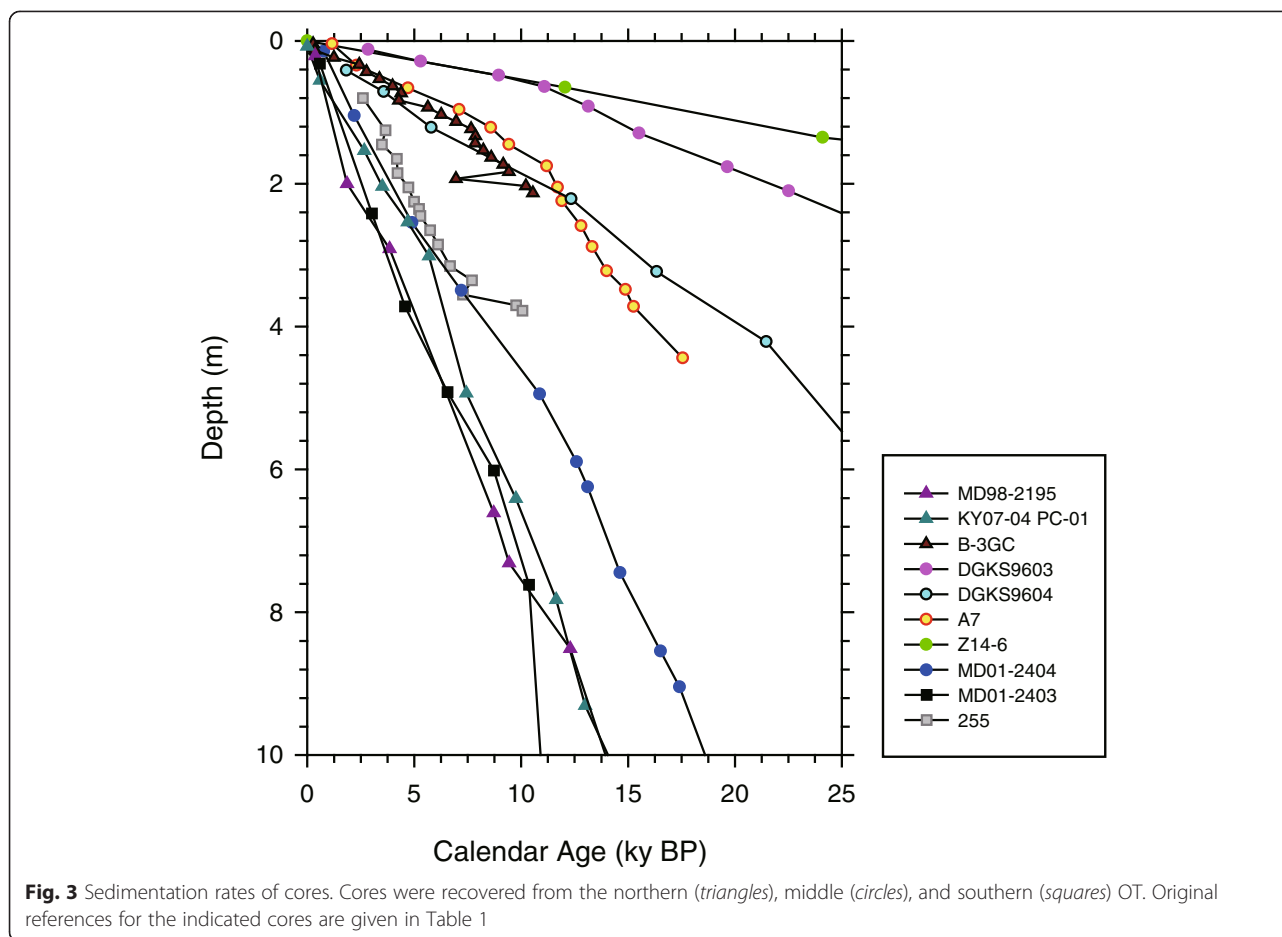
Kim et al. Progress in Earth and Planetary Science (2015) 2:43

Page 5 of 16

Table 1 Information on marine sediment cores of the OT used for past SST reconstructions

Proxy	Core	Latitude, longitude	Water depth (m)	Age control		Reservoir age (y)	CALIB version	Time resolution (y)	Sedimentation rate (cm/ky)		Observed SST[a] (°C)	Core-top proxy temp. (°C)	Average temperature (°C)		Calibration equation	Reference
				Method	Foraminiferal species				Late Holocene	LGM			Late Holocene	LGM		
U$^{K'}_{37}$	Z14-6	27° 07' N 127° 27' E	739	$\delta^{18}O$	*Globigerinoides sacculifer* *Neogloboquadrina dutertrei*	–	–	1000	5.4	5.8	25.0	–	26.3 ± 0.4	24.4 ± 0.6	Müller et al. (1998)	Zhou et al. (2007)
	DGKS 9604	28° 17' N 127° 01 'E	766	^{14}C	*Neogloboquadrina dutertrei* *Planktonic foraminifer mixture* (1071–1074 cm)	–	4.4	100–300	20.4	19.1	25.6	26.2	26.1 ± 0.4	22.7 ± 0.4	Müller et al. (1998)	Yu et al. (2009)
	KY07-04 PC-01	31° 38' N 128° 57' E	758	^{14}C	*Neogloboquadrina dutertrei*	–	5.0	50–200	55.3	–	22.3	22.3	23.8 ± 0.4	–	Prahl et al. (1988)	Nakanishi et al. (2012a)
	MD98-2195	31° 38' N 128° 57' E	746	^{14}C	*Globigerina bulloides* *Neogloboquadrina dutertrei*	400	4.3	125	66.1	74.2	22.3	23.9	23.7 ± 0.5	20.1 ± 0.8	Prahl et al. (1988)	Ijiri et al. (2005)
Mg/Ca	MD01-2403	25.3° N 123.2° E	1420	^{14}C	*Globigerinoides* spp. *Orbulina universa*	400	5.0	~70	85.4	–	27.5	27.6	28.0 ± 0.6	–	Hastings et al. (2001)	Lin et al. (2006)
	MD01-2404	26° 39' N 125° 49' E	1397	^{14}C $\delta^{18}O$	*Globigerinoides ruber* *Globigerinoides sacculifer* *Uvigerina* spp.	400 –	6.0 –	68–373	53.6	52.4	27.1	26.9	27.1 ± 0.7	24.3 ± 0.7	Hastings et al. (2001)	Chen et al. (2010)
	KH13-4-HR2MC	27° 40' N 127° 23' N	1675	Core-top sediment				–	–	–	26.8	26.7	–	–	Hastings et al. (2001)	Horikawa et al. (2015)
	A7	27° 49' N 126° 59' E	1264	^{14}C	*Neogloboquadrina dutertrei*	700	5.0	22–150	18.2	–	27.2	–	26.6 ± 0.6	–	Hastings et al. (2001)	Sun et al. (2005)
Foram. Assem[b]	KY07-04 PC-01	31° 38' N 128° 57' E	758	^{14}C	*Neogloboquadrina dutertrei*	–	5.0	50–200	55.3	102.0	24.9	24.9	25.9 ± 0.9	21.8 ± 1.1	FP-12E, SIMMAX28	Jian et al. (2000)
	255	25° 12' N 123° 07' E	1575	^{14}C	*Neogloboquadrina dutertrei*	–	–	185	59.4	-	Aug. 28.9	(29.0/ 28.8)[c]	(28.8 ± 0.3/ 28.8 ± 0.1)[c]	–	FP-12E, SIMMAX28	Jian et al. (2000)
											Feb. 23.3	(24.3/ 24.3)[c]	(24.3 ± 0.9/ 23.9 ± 1.2)[c]	–		
	MD01-2404	26° 39' N 125° 49' E	1397	^{14}C	*Globigerinoides ruber* *Globigerinoides sacculifer*	400	5.0	62–202	53.9	48.5	Aug. 28.9	28.6	28.6 ± 0.1	27.9 ± 0.6	RAM	Chang et al. (2008)
											Feb. 22.5	23.3	23.4 ± 0.8	22.5 ± 1.2		
	DGKS 9603	28°09' N 127° 16' E	1100	^{14}C	*Globorotalia menardii* *Globigerinoides sacculifer* *Neogloboquadrina dutertrei*	400	4.1	46–474	4.0	11.6	Aug. 29.0	27.7	28.5 ± 0.4	27.1 ± 0.4	MAT	Li et al. (2001)

Table 1 Information on marine sediment cores of the OT used for past SST reconstructions *(Continued)*

										Feb.	22.1	25.0	25.5 ± 0.4	24.0 ± 0.6	
B-3GC	31° 29' N 128° 31' E	555	^{14}C	*Neogloboquadrina dutertrei*	–	–	130	10.3	–	Aug.	28.4	(27.9/28.1)[c]	(28.4 ± 0.3/28.5 ± 0.4)[c]	–	FP-12E, SIMMAX28	Jian et al. (2000)
										Feb.	17.7	(19.1/21.3)[c]	(20.3 ± 1.0/22.6 ± 1.8)[c]	–	

[a]Temperature data from the JODC datacenter (http://www.jodc.go.jp). Temperatures for the alkenone proxy are the annual mean temperatures at depths of 0–30 m; those for the Mg/Ca proxy are June–November mean temperatures at depths of 0–50 m; and those for the summer and winter assemblage-based temperatures are August and February temperatures at 0 m, respectively [b]Foraminiferal assemblage [c]Numbers in parenthesis refer to assemblage-based temperatures reconstructed using FP-12E and SIMMAX-28, respectively

Kim *et al. Progress in Earth and Planetary Science* (2015) 2:43

Page 7 of 16

Fig. 3 Sedimentation rates of cores. Cores were recovered from the northern (*triangles*), middle (*circles*), and southern (*squares*) OT. Original references for the indicated cores are given in Table 1

mean SST. According to another study on alkenones and alkyl alkenoate fluxes from time-series sediment traps installed in the northwestern Pacific Ocean from March 1991 until March 1992 (Sawada et al. 1998), there was no seasonality in the alkenone flux in deep water. In a trap close to the surface, the fluxes were high (up to 16.5 μg/m^2·day) for the July–August period but dropped to less than 6 μg/m^2·day for the remaining experimental duration. However, in sediment traps suspended close to the bottom, fluxes remained constant (less than 6 μg/m^2·day) in all seasons. In addition, Sawada et al. (1998) compared the $U^{K'}_{37}$ of core-top sediments with that of time-series sediment trap samples and found them to be in good agreement with annual mean $U^{K'}_{37}$. Therefore, it seems that the alkenone-based temperature represents the annual mean temperature in the OT.

Core-top alkenone-based temperatures
To examine whether the alkenone-based temperatures reconstructed from marine sediments represent the SST, alkenone-based temperatures estimated using core-top samples were compared with annual mean temperatures

at water depths of 0–30 m (Fig. 4a, b). The reason this maximum water depth (approximately 30 m) was chosen is that a study on the depth variation of the alkenone concentration shows that maximum concentration occurs in the top 25 m of the water column (Nakanishi et al. 2012b). Annual mean temperatures were obtained from the Japan Oceanographic Data Center (JODC, http://www.jodc.go.jp) and were observed from 1906 to 2003. Core-top temperatures were calculated from sediments collected from the tops of cores KY07-04 PL-01, MD98-2195, and DGKS9604. There is no core-top sediment in core Z14-6. Core KY07-04 PL-01 was recovered using a multiple coring device along with core KY07-04 PC-01. Core-top sediment collected from the multiple core was used to reconstruct the alkenone-based temperature because core-top sediment was missing in core KY07-04 PC-01 (Nakanishi et al. 2012a). Annual mean temperatures of 22.3, 22.3, and 25.6 °C (water column depths of 0–30 m, JODC data) corresponded with core-top alkenone-based temperatures of 22.3, 23.9, and 26.2 °C, which were calculated using cores KY07-04 PL-01, MD98-2195, and DGKS9604, respectively. Thus, the temperatures reconstructed using core-top sediments
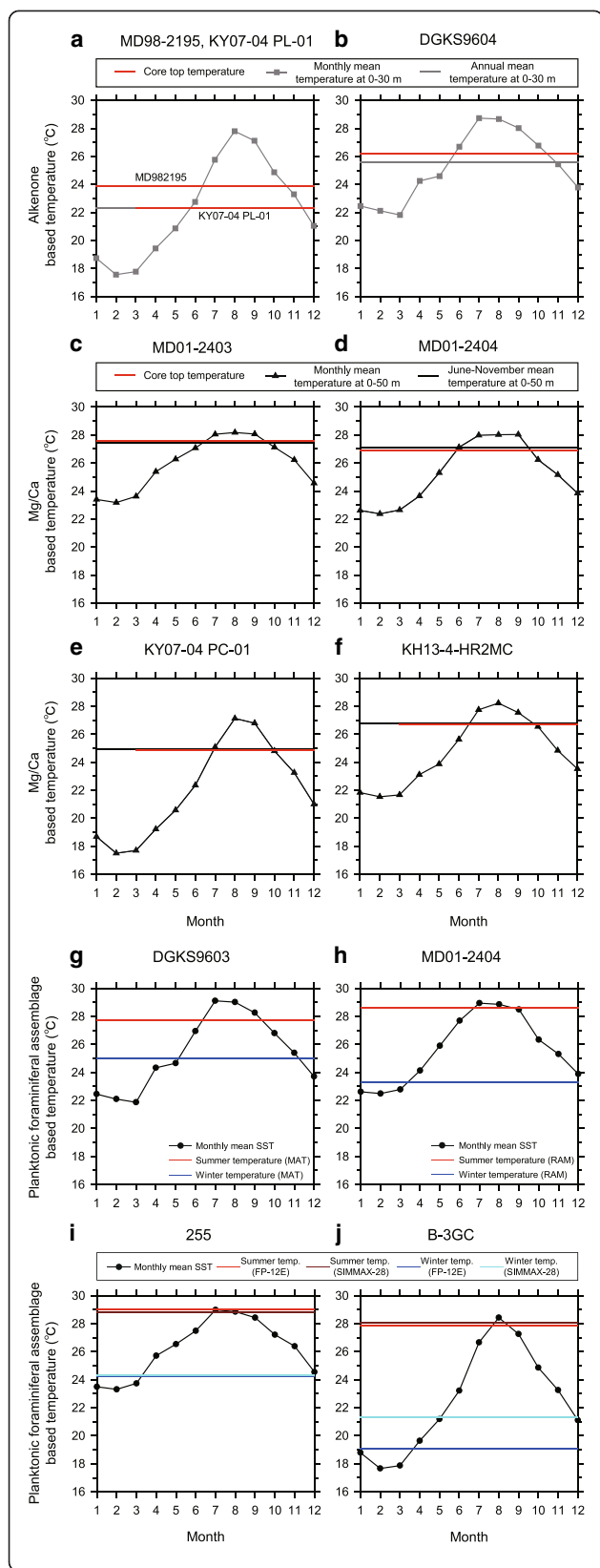
Kim *et al. Progress in Earth and Planetary Science* (2015) 2:43

Page 8 of 16

Fig. 4 Comparisons of observed temperatures (JODC database) with corresponding core-top temperatures reconstructed using various proxies. The investigated proxies are alkenones (**a**, **b**), Mg/Ca (**c**–**e**), and foraminiferal assemblages (**f**–**i**). Original references for the indicated cores are given in Table 1

were within 0.6 °C of the annual mean surface water temperatures at each location, except for that of core MD98-2195, in which the core-top estimate was over 1 °C warmer. This suggests that alkenone-based temperatures reconstructed from core-top sediments can represent the annual mean SST.

Foraminiferal Mg/Ca ratio
The Mg/Ca ratio of planktonic foraminiferal calcite can also be used as a proxy for the SST because it changes with seawater temperature (Nürnberg et al. 1996). Many different calibration equations can be used to convert Mg/Ca to SSTs (e.g., Nürnberg et al. 1996; Elderfield and Ganssen 2000; Dekens et al. 2002; Anand et al. 2003). The equation below (equation 4) has been used extensively to reconstruct SSTs in the OT (Sun et al. 2005; Lin et al. 2006; Chen et al. 2010; Kubota et al. 2010). This equation was derived by Hastings et al. (2001) from studies that related core-top Mg/Ca of *G. ruber* to observed SSTs in the South China Sea:

$$T = \ln((Mg/Ca)/0.38)/0.089. \qquad (4)$$

Habitat depth of G. ruber
Investigations of foraminiferal distributions in the Pacific, Atlantic, and Indian Oceans have suggested that 75–100 % of *G. ruber* live at water depths of 0–40 m (van Donk 1977). Furthermore, according to studies on the oxygen isotope ratios of *G. ruber*, the habitat depth of *G. ruber* is 2–50 m in the South China Sea and 40 m in the region southwest of Taiwan (Lin et al. 2004; Lin 2014). Therefore, Mg/Ca of *G. ruber* are likely to record temperatures at depths of 0–50 m in the water column.

Seasonality of G. ruber
G. ruber is a tropical/subtropical species that is most abundant in warm waters (Bé and Tolderlund 1971; Bijma et al. 1990). Hence, the temperatures calculated using the Mg/Ca of *G. ruber* are thought to represent summer temperatures in the OT (Sun et al. 2005; Lin et al. 2006; Chen et al. 2010; Kubota et al. 2010). Xu et al. (2005) examined the *G. ruber* flux from time-series sediment traps installed in the middle region of the OT from October 1994 to August 1995 (at station JAST01, Fig. 1). According to this study, the relative

Kim *et al. Progress in Earth and Planetary Science* (2015) 2:43

Page 9 of 16

abundance of *G. ruber* was 20 % of the total foraminiferal species during the summer to autumn period but declined to 5 % in winter. Yamasaki and Oda (2003) also examined *G. ruber* fluxes from time-series sediment traps installed in the mid region of the OT from March 1993 to February 1994 (at station SST2, Fig. 1). They found that the *G. ruber* flux from summer to autumn was approximately three times higher than that in winter both at the sediment trap close to the surface and that close to the seafloor. Thus, it is likely that Mg/Ca-based temperatures of *G. ruber* represent summer to autumn (June–November) temperatures in the OT.

Mg/Ca-based core-top temperatures

To examine whether the Mg/Ca-based temperatures of marine sediments represent SSTs, core-top temperatures reconstructed using Mg/Ca were compared with observed summer to autumn (June–November) mean water temperatures at depths of 0–50 m from the JODC database (Fig. 4c–f). The reason this maximum water depth (approximately 50 m) was chosen is that the habitat depth of *G. ruber* is considered to be in this range. Core-top Mg/Ca-based temperatures from cores MD01-2403, MD01-2404, KY07-04 PC-01, and KH13-4-HR2MC4 were compared. The reconstructed core-top Mg/Ca-based temperatures of 27.6, 26.9, 24.9, and 26.7 °C closely match the observed mean temperatures of 27.5, 27.1, 24.9, and 26.8 °C, respectively (June–November, water depths of 0–50 m, JODC database). Thus, temperatures reconstructed using the Mg/Ca ratio of *G. ruber* are consistent with summer to autumn SSTs in the OT.

Foraminiferal assemblages

Data on planktonic foraminiferal assemblages can be converted into temperature estimates by statistical processing. Four statistical estimation techniques were used to reconstruct temperatures for the OT (Table 1). The temperature estimates obtained using these different statistical techniques are compared here.

Estimation techniques

Past February and August SSTs for the OT were reconstructed from planktonic foraminiferal assemblage data using four estimation techniques: the modern analog technique (MAT), the revised analog method (RAM), a modern analog technique using a similarity method (SIMMAX-28), and FP-12E (Table 1). The MAT uses a dissimilarity index to select core-top sediments that have foraminiferal assemblages similar to the foraminiferal assemblages of obtained samples (Prell 1985). The RAM is derived from the MAT (Waelbroeck et al. 1998). Waelbroeck et al. (1998) suggested that the

RAM minimizes the uncertainty and bias of foraminiferal SST estimates. SIMMAX uses a similarity index to select core-top sediments that have similar assemblages (Pflaumann et al. 1996). SIMMAX-28 was developed to reconstruct the temperature in the western Pacific and is derived from SIMMAX (Pflaumann and Jian 1999). FP-12E was developed from the Imbrie and Kipp transfer function method (IKM) and is appropriate for reconstructing the temperature of the northwestern Pacific region (Thompson 1981). In the IKM, foraminiferal species are classified into several groups based on their characteristics, and the SSTs are then estimated using a transfer function process (Imbrie and Kipp 1971).

Foraminiferal assemblage-based core-top temperatures

The planktonic foraminiferal assemblage technique is based on the compositional change in the foraminiferal assemblage with changing water temperature (Prell 1985). Past February and August SSTs can be reconstructed from this proxy. To examine whether foraminiferal assemblage-based temperatures of marine sediments are consistent with current SSTs, core-top August and February assemblage-based temperatures were compared with observed (JODC database, surface water) temperatures in August and February (Fig. 4g–j).

The assemblage-based temperature of core DGKS9603 (middle OT) was reconstructed using the MAT (Fig. 4g) (Li et al. 2001). The August assemblage-based temperature of the core-top sediment was 27.7 °C, which was 1 °C colder than the observed SST for August (29.0 °C). Thus, the foraminiferal temperature agreed well with the observed August SST considering the margin of error of ±1.50 °C (Ortiz and Mix 1997). In contrast, the February assemblage-based temperature of the core-top sediment was 25.0 °C, which was 3 °C warmer than the observed February SST (22.1 °C). Thus, the assemblage-based temperature estimated using the MAT was not consistent with the observed February SST for this core considering the margin of error of ±1.50 °C (Ortiz and Mix 1997).

The August and February SSTs were reconstructed from core MD01-2404 (middle OT) using the RAM (Fig. 4h) (Chang et al. 2008). The August and February assemblage-based temperatures of the core-top sediment were 28.6 and 23.3 °C, respectively, which were consistent with the respective observed SSTs for August (28.9 °C) and February (22.5 °C) within the margins of error of ±0.72 °C for summer and ±1.17 °C for winter (Table 2). Therefore, foraminiferal assemblage-based temperatures estimated using the RAM from the MD01-2404 core-top represent the observed SSTs.

Core 255 assemblage-based temperatures were reconstructed using both FP-12E and SIMMAX-28 (Fig. 4i) (Jian et al. 2000). The assemblage summer core-top

Kim *et al. Progress in Earth and Planetary Science* (2015) 2:43

Page 10 of 16

Table 2 Comparison of errors in foraminiferal assemblage-based temperature estimates calculated using four techniques

Method	Core	SST	Estimation error (°C)[a]	Calibration dataset
MAT	DGKS9603	Summer	±1.50	Global
		Winter		
RAM	MD01-2404	Summer	±0.72	Western Pacific
		Winter	±1.17	
SIMMAX-28	255 B-3GC	Summer	±0.45	Western Pacific
		Winter	±1.27	
FP-12E	255 B-3GC	Summer	±1.46	Northwestern Pacific
		Winter	±2.48	

[a]Studies in which estimation errors are defined: MAT (Ortiz and Mix 1997), RAM (Chen et al. 2005), SIMMAX-28 (Pflaumann and Jian 1999), and FP-12E (Thompson 1981)

temperature estimates obtained using FP-12E and SIMMAX-28 were 29.0 and 28.8 °C, respectively, both of which were consistent with the observed August SST (28.9 °C) within the margins of error of ±1.46 °C for FP-12E and ±0.45 °C for SIMMAX-28. The assemblage winter temperatures were estimated to be 24.3 °C using both techniques (FP-12E error; ±2.48 °C, SIMMAX-28 error; ±1.27 °C, Table 2). Considering the margins of error, this estimated temperature was consistent with the observed February SST (23.3 °C) for core 255 for both techniques.

Core B-3GC assemblage-based temperatures were also reconstructed using both FP-12E and SIMMAX-28 (Fig. 4j) (Jian et al. 2000). The August assemblage-based temperatures were 27.9 °C (FP-12E) and 28.1 °C (SIM-MAX-28), both of which were close to the observed August SST (28.4 °C). The February assemblage-based temperatures were 19.1 °C (FP-12E) and 21.3 °C (SIM-MAX-28), whereas the observed February SST was 17.7 °C. Considering the error ranges (FP-12E; ±2.48 °C, SIMMAX-28; ±1.27 °C, Table 2), the temperature estimated using FP-12E is consistent with the observed February SST, but that estimated using SIMMAX-28 is not. Hence, the summer assemblage-based temperatures reconstructed from core-top sediments using either technique may represent the observed August SST (Fig. 4g–j). However, reconstructed winter assemblage-based temperatures may be somewhat higher than the observed February SST if SIMMAX-28 is used.

In summary, if these results were expanded and assumed to apply to other cores, the RAM appears to be the most accurate statistical technique for estimating August and February SSTs using the foraminiferal assemblage proxy for core-top sediments from the OT.
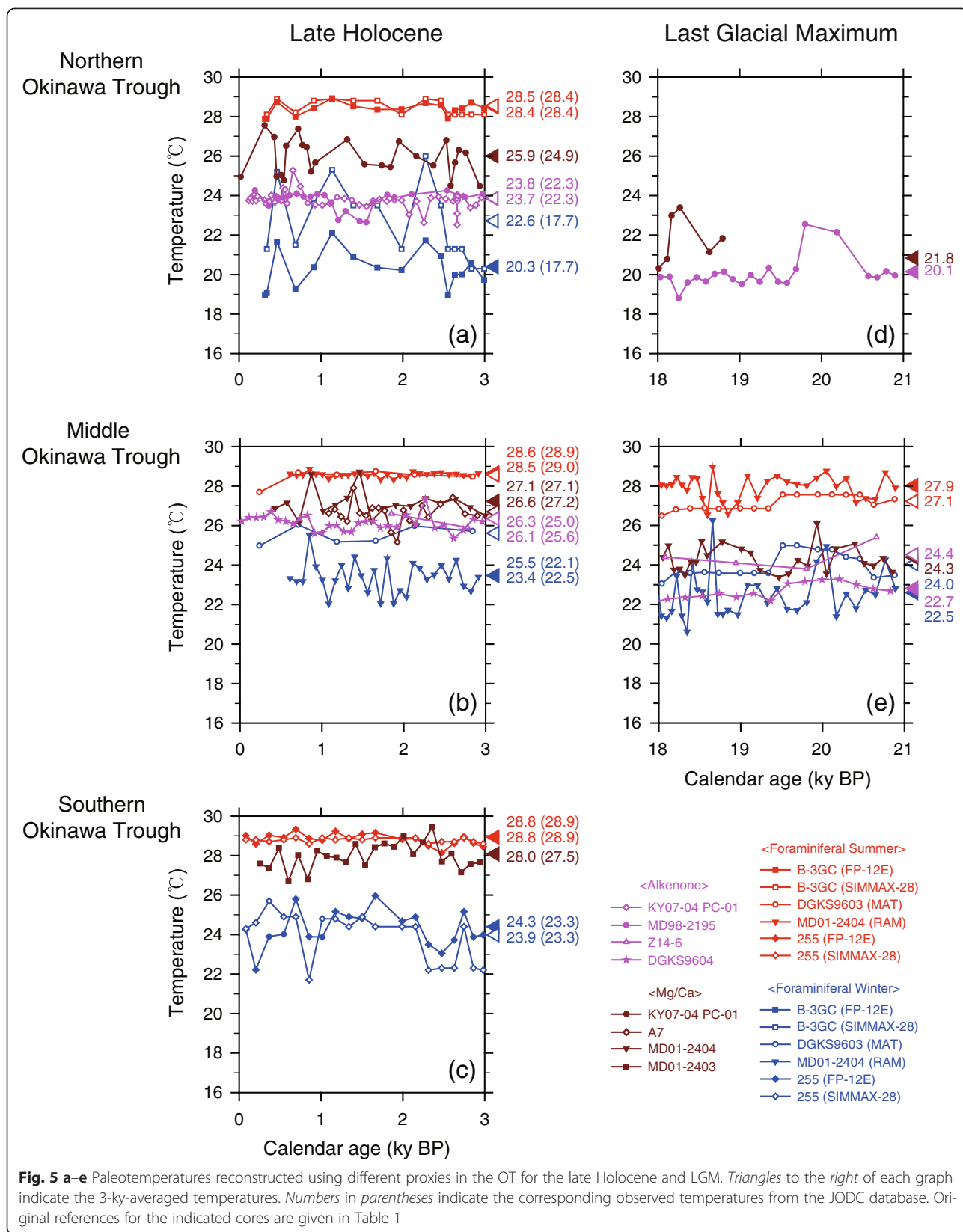
Paleotemperature estimates

Late Holocene (0–3 cal ky BP)

We compared observed current SSTs (JODC database) to 3-ky-averaged (late Holocene) paleotemperatures reconstructed from marine sediments using alkenone, Mg/Ca ratio, and foraminiferal assemblage proxies (Fig. 5a–c).

In the northern OT (Fig. 5a), the reconstructed alkenone-based temperatures of cores KY07-04 PC-01 and MD98-2195 for the late Holocene were 23.8 ± 0.4 and 23.7 ± 0.5 °C, respectively. These paleotemperature estimates are approximately 1.5 °C higher than the observed annual mean SST (22.3 °C). According to a comparison of alkenone-based temperatures estimated from different 24 laboratories (Rosell-Melé et al. 2001), the precision of alkenone-based temperature estimates is approximately ±1.6 °C within a 95 % confidence level. We therefore suggest that reconstructed alkenone-based temperatures in the northern OT represent annual mean SSTs. In the middle OT (Fig. 5b), the 3-ky-averaged alkenone-based temperatures of cores Z14-6 and DGKS9604 were 26.3 ± 0.4 °C and 26.1 ± 0.4 °C, respectively. These paleotemperatures appear to be approximately 1 °C warmer than current annual mean SSTs (25.0 and 25.6 °C, respectively), but given the margin of error of alkenone-based temperatures (±1.6 °C) (Rosell-Melé et al. 2001), they do in fact represent the annual mean SSTs.

The Mg/Ca-based temperature of core KY07-04 PC-01 (northern OT, Fig. 5a) during the late Holocene was 25.9 ± 0.9 °C; considering the margin of error (±1–2 °C) (Rosenthal et al. 2004), this can represent the observed June–November mean SST (24.9 °C). The Mg/Ca-based paleotemperatures of cores MD01-2404 and A7 (middle OT, Fig. 5b) were 27.1 ± 0.7 and 26.6 ± 0.6 °C, respectively, which are similar to the observed June–November mean SSTs (27.1 and 27.2 °C, respectively) when considering the margin of error for Mg/Ca-based temperatures. In the southern OT (Fig. 5c), the Mg/Ca-based paleotemperature of MD01-2403 is 28.0 ± 0.6 °C, which can represent the observed June–November mean temperature (27.5 °C), given the error range.

August paleo-SSTs obtained from the planktonic foraminiferal assemblage of core B-3GC (northern OT, Fig. 5a) were 28.5 ± 0.4 °C (SIMMAX-28) and 28.4 ± 0.3 °C (FP-12E). These paleotemperatures are consistent with the observed SST (28.4 °C). In contrast, the February assemblage-based paleotemperatures are not consistent with the observed SST. The February assemblage-based paleo-SSTs of core B-3GC were 22.6 ± 1.8 °C (SIMMAX-28) and 20.3 ± 1.0 °C (FP-12E). Taking into account the margins of error of SIMMAX-28 (±1.27 °C) (Pflaumann and Jian 1999) and FP-12E (±2.48 °C) (Thompson 1981), the February assemblage SSTs are inconsistent with the observed SST (17.7 °C), as they were 4.9 and 2.6 °C warmer than the observed SST, respectively.
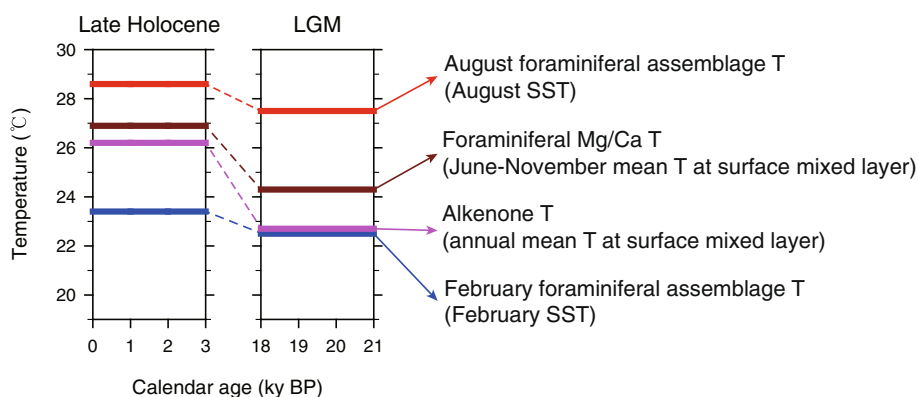
Kim *et al. Progress in Earth and Planetary Science* (2015) 2:43

Page 11 of 16

Fig. 5 a–e Paleotemperatures reconstructed using different proxies in the OT for the late Holocene and LGM. *Triangles* to the *right* of each graph indicate the 3-ky-averaged temperatures. *Numbers* in *parentheses* indicate the corresponding observed temperatures from the JODC database. Original references for the indicated cores are given in Table 1

Kim *et al. Progress in Earth and Planetary Science* (2015) 2:43

Page 12 of 16

Fig. 6 Schematic diagram of SST proxy data in the OT. SST proxy data are given for periods during the late Holocene (0–3 cal ky BP) and LGM (18–21 cal ky BP). *T* indicates temperature

The August assemblage-based paleo-SSTs of cores MD01-2404 and DGKS9603 (middle OT, Fig. 5b) were 28.6 ± 0.1 and 28.5 ± 0.4 °C, respectively. Considering the error ranges of ±0.72 °C for the RAM (Chen et al. 2005) and ±1.50 °C for the MAT (Ortiz and Mix 1997), the assemblage-based paleo-SSTs are close to the observed SSTs (28.9 and 29.0 °C for cores MD01-2404 and DGKS9603, respectively). In contrast, the February assemblage-based paleo-SSTs are not consistent with the observed SSTs. The February assemblage-based paleotemperature of core MD01-2404 is 23.4 ± 0.8 °C, which is consistent with the observed SST (22.5 °C) within the margin of error (±1.17 °C) (Chen et al. 2005). However, overall, the winter paleo-SSTs are mostly warmer than the observed SSTs, as seen in cores from the middle OT.

The August assemblage-based paleo-SSTs of core 255 (southern OT, Fig. 5c) were 28.8 ± 0.3 °C (FP-12E) and 28.8 ± 0.1 °C (SIMMAX-28). The margins of error for the two techniques are ±1.46 °C (FP-12E) and ±0.45 °C (SIMMAX-28, Table 2). Thus, the summer assemblage-based paleo-SSTs for core 255 agree well with the observed August SST (28.9 °C). In contrast, the February assemblage-based paleo-SSTs are 24.3 ± 0.9 °C (FP-12E) and 23.9 ± 1.2 °C (SIMMAX-28), which are 1 and 0.6 °C warmer than the observed February SST (23.3 °C), respectively, which are within the margins of error (FP-12E; ±2.48 °C, SIMMAX-28; ±1.27 °C, Table 2).

In summary, the SSTs reconstructed for the late Holocene from various proxies were compared with present observed SSTs from the JODC database. During the late Holocene, the alkenone- and Mg/Ca-based temperatures represent the present annual and summer to autumn mean SSTs, respectively. In addition, the assemblage-based summer paleo-SSTs were consistent with the present August SST, but the assemblage-based winter paleo-SSTs were usually higher than the present

February SST. However, the winter SSTs deviated furthest from the present SSTs in the northern OT, and the assemblage-based paleotemperature estimates gradually moved closer to the present SSTs with increasing southerly core locations.

Last glacial maximum (18–21 cal ky BP)
We compared 3-ky-averaged temperatures reconstructed from alkenone, Mg/Ca, and foraminiferal assemblage proxies during the late Holocene (0–3 cal ky BP) with SSTs during the LGM (18–21 cal ky BP), when the climate was dramatically different from the present-day climate (Fig. 5).

In the northern OT (Fig. 5a, d), the alkenone-based temperature of core MD98-2195 was 20.1 ± 0.8 °C during the LGM, which is 3.6 °C cooler than the late Holocene alkenone-based temperature. Although only 1000 y of Mg/Ca-based temperature data exist for core KY07-04 PC-01 during the LGM, this core appears to have been 4.1 °C cooler during the LGM than during the late Holocene. Foraminiferal assemblage-based temperatures could not be compared because there are no data during the LGM.

In the middle OT (Fig. 5b, e), the alkenone-based temperatures of cores Z14-6 and DGKS9604 during the LGM were 24.4 ± 0.6 and 22.7 ± 0.4 °C, respectively, which are 1.9 and 3.4 °C colder than their respective alkenone-based temperatures during the late Holocene. The Mg/Ca-based temperature of core MD01-2404 is 24.3 ± 0.7 °C, which is 2.8 °C colder than that during the late Holocene. The August assemblage SSTs of cores MD01-2404 and DGKS9603 were 27.9 ± 0.6 and 27.1 ± 0.4 °C, respectively, which are 0.7 and 1.4 °C colder than their respective late Holocene temperatures. The February assemblage SSTs of cores MD01-2404 and DGKS9603 during the LGM were 22.5 ± 1.2 and 24.0 ± 0.6 °C, respectively, which are also 0.9 and

1.4 °C colder than during the late Holocene. There are no data on temperature proxies in the southern OT during the LGM.

Overall, comparisons of proxy temperatures between the two periods suggest that SSTs during the LGM were lower than those during the late Holocene. However, the magnitudes of the temperature differences are dependent on the proxy. The alkenone- and Mg/Ca-based temperatures were 3–3.5 °C lower in the LGM than in the late Holocene, whereas February and August assemblage SSTs were only 1–1.2 °C lower in the LGM than in the late Holocene.

Comparisons between sea surface temperature proxies

There is a SST gradient between the southern, middle, and northern OT. The middle OT is the region where most temperature data could be obtained from the three proxies used for paleotemperature reconstructions (Fig. 5). Hence, we compared the reconstructed SSTs obtained using proxies in the middle OT.

First, alkenone-based temperatures were compared with Mg/Ca-based temperatures. Alkenone-based temperatures were lower (approximately 1 °C) than Mg/Ca-based temperatures during the late Holocene. During the LGM, alkenone-based temperatures were again lower than Mg/Ca-based temperatures. This seems reasonable because the alkenone-based temperature represents the annual mean temperature, whereas the Mg/Ca-based temperature represents the summer to autumn temperature. At present, the annual mean temperature is lower than the summer to autumn temperature in the area. In addition, water temperatures at the surface are almost the same as those in the depth ranges of 0–30 and 0–50 m in the study area (JODC dataset, 1906–2003). Hence, both alkenone- and *G. ruber* Mg/Ca-based temperatures represent the SST.

Second, Mg/Ca-based temperatures were compared with August and February assemblage-based temperatures. Because the core-top and 3 ky average February temperatures of core DGKS9603 were approximately 3 °C warmer than the present February SST, this core was excluded from the comparison. During the late Holocene, Mg/Ca-based temperatures of cores A7 and MD01-2404 were 26.6 and 27.1 °C, respectively, which are 1.5–2 °C colder than summer assemblage SSTs of MD01-2404 and DGKS9603 (28.6 °C) and 3.2–3.7 °C warmer than the winter SST of MD01-2404 (23.4 °C). The lower Mg/Ca-based temperatures compared to the summer assemblage-based temperatures appear to be reasonable because the Mg/Ca-based temperature represents the summer to autumn temperature. During the LGM, the Mg/Ca-based temperature of MD01-2404 (24.3 °C) was colder than the summer assemblage SSTs of cores MD01-2404 and DGKS9603 (27.9 and 27.1 °C, respectively). In

contrast, the Mg/Ca-based temperature of MD01-2404 (24.3 °C) is close to the winter SST (22.5 °C), considering the margin of error (±1–2 °C) (Rosenthal et al. 2004).

Third, alkenone-based temperatures were compared with the August and February assemblage SSTs. During the late Holocene, alkenone-based temperatures of cores Z14-6 and DGKS9604 were 26.3 and 26.1 °C, respectively, which are approximately 2.4 °C colder than the summer assemblage SSTs of cores MD01-2404 and DGKS9603 (approximately 28.6 °C) and approximately 2.8 °C warmer than the winter SST of core MD01-2404 (23.4 °C). During the LGM, the alkenone-based temperatures of cores Z14-6 and DGKS9604 were 24.4 and 22.7 °C, respectively, which are approximately 3–5 °C colder than their summer assemblage SSTs (27.9 °C) but close to the winter assemblage SST of core MD01-2404 (22.5 °C).

In summary, the August assemblage SSTs were the warmest among the three proxy SSTs during both the late Holocene and the LGM. The February assemblage SSTs were lower than the alkenone- and Mg/Ca-based temperatures during the late Holocene but close to the two other proxy temperatures during the LGM. It is possible that the warm February assemblage SSTs are caused by the uncertainty in estimating the foraminiferal assemblage-based temperatures.

Hydrographic change of the Okinawa Trough and climatological implications
Last glacial maximum

The hydrography of the East China Sea is largely controlled by the path and strength of the KC and the intensity of the Asian summer monsoon. During the LGM, when sea level was lowered by approximately 130 m (Waelbroeck et al. 2002), large areas of the continental shelf in the East China Sea were exposed to air. The coastline of China and the OT were closer than they are today, and consequently, the OT might be directly affected by the freshwater that was discharged from the paleoriver during the LGM. The high sedimentation rates in the OT during this period were probably due to the increased supply of terrigenous sediments through the river (Fig. 3). The high abundance of *Neogloboquadrina pachyderma*, *Neogloboquadrina incompta*, and *Globigerina quinqueloba* supports the presumption that cold, low-saline water was discharged into the northern OT during the LGM (Ijiri et al. 2005). In addition, the glacial SSS reconstructed using the alkenone-based SST and *Globigerinoides sacculifer* $\delta^{18}O$ was lower than that of today, indicating the possibility of the influence of freshwater discharge on the ECS during the LGM (Yu et al. 2009).

There are two hypotheses regarding the KC in the OT during the LGM. One is that the KC flowed into the OT

Kim *et al. Progress in Earth and Planetary Science* (2015) 2:43

Page 14 of 16

during the glacial but the intensity of current was weakened (Xu and Oda 1999). The other is that the inflow of the KC into the OT was prohibited by the formation of a land bridge between Taiwan and the southern Ryukyu Arc and thus it flowed along the eastern side of the Ryukyu Islands (Ujiié et al. 2003; Kao et al. 2006). However, a recent study on the geochemical proxy records of marine sediment cores recovered from inside and outside the OT shows no significant difference in the glacial SST and the planktonic foraminiferal $\delta^{18}O$ between the OT and the Ryukyu forearc (Lee et al. 2013). This indicates that the glacial SST and salinity were almost same inside and outside the OT. Hence, during the glacial period, Kuroshio water most likely flowed into the OT and along the shelf break until it drained out through the Tokara Strait.

Deglaciation

The deglaciation period is the transitional period between the glacial and the Holocene when the sea level began to rise rapidly. Deglacial records of the planktonic $\delta^{18}O$- and Mg/Ca-based SSTs from the middle OT show that SSTs were 3 °C cooler and the SSSs were 1 psu saltier at 18–17 cal ky BP than today (Sun et al. 2005). Based on the data, Sun et al. (2005) suggested that the influence of the summer East Asian monsoon was weaker in the past than it is today. According to them, the timing of suborbital SST oscillations was closely linked with abrupt changes in the East Asian monsoon system and the North Atlantic climate at 16–12 cal ky BP.

The SST of the OT increased sharply with the onset of the late deglaciation between 16–15 cal ky BP. *Pulleniatina obliquiloculata* and *G. sacculifer* species, which prefer warm water, began to appear in the middle OT at that time, suggesting that the surface seawater of the OT started to warm up (Li et al. 2001). Saline surface water dominated over the middle OT during 16–12 cal ky BP, indicating that the strength of the Kuroshio increased at that time (Yu et al. 2009). Conversely, according to other studies (Wang et al. 2001; Yuan et al. 2004), the $\delta^{18}O$ of stalagmites from Chinese caves was isotopically light during the late deglaciation, indicating that precipitation increased because of the increased strength of the East Asian summer monsoon at that time.

The Younger Dryas climate event (YD) was identified in the northern and middle OT based on the SST patterns reconstructed using the Mg/Ca ratio of planktonic foraminifera (Sun et al. 2005; Chen et al. 2010; Kubota et al. 2010). It occurred from 12.5 to 11.8 cal ky BP in the northern OT (Kubota et al. 2010). The timing of the YD is consistent with the time when the $\delta^{18}O$ of stalagmites from the Hulu and Dongge caves was high (Wang et al. 2001; Yuan et al. 2004). This suggests that the

climate of the northwestern Pacific and the North Atlantic were connected via atmospheric circulation (Chen et al. 2010).

Holocene

Millennial-scale variations between warmer, more saline and cooler, less saline surface water during the deglaciation and the Holocene were identified from the core located in the northern OT (Kubota et al. 2010). Kubota et al. (2010) correlated these millennial-scale variations to changes in the mixing ratio between the Kuroshio water and the diluted Changjiang (Yangtze) water. In particular, the East Asian summer monsoon precipitation events identified from the SSS records of the northern OT agree with the maxima in the $\delta^{18}O$ records of stalagmites from various parts of the Changjiang River drainage (e.g., Kubota et al. 2010). These events are also in good agreement with North Atlantic ice-rafted events, suggesting a teleconnection between the North Atlantic climate and the East Asian summer monsoon during the Holocene.

The *Pulleniatina* Minimum Event (PME) occurred during the period of 4.5–3 cal ky BP and is characterized by a low abundance of the species *P. obliquiloculata*, which is an indicator of the KC (e.g., Ujiié et al. 2003; Lin et al. 2006). Previous studies suggest that the low abundance of *P. obliquiloculata* during the PME is associated with changes in the climate and ocean environment (Jian et al. 2000; Li et al. 2001; Ujiié et al. 2003; Lin et al. 2006). However, the causes of this phenomenon are still being debated. Jian et al. (2000) reconstructed the SST changes using foraminiferal assemblages and recovered variation in the past thermocline depth in the northern and southern OT. They suggested that the winter monsoon had been strengthened during the PME. Conversely, Ujiié et al. (2003) and Lin et al. (2006) suggested that the SST in the middle and southern OT did not decrease at that time, and the abundance of planktonic foraminifera, which prefer cold water, in the same region, also did not increase during the PME. Ujiié et al. (2003) suggested that the El Niño-like conditions in the equatorial Pacific resulted in a reduced KC, which might be related to the lower rate of primary productivity, ultimately resulting in the low abundance of *P. obliquiloculata*. However, Lin et al. (2006) suggested that the primary productivity did not change significantly during the PME in the southern OT.

Conclusions

Alkenones were found to be most abundant at depths of 0–30 m in the water column of the OT and were produced in all seasons. *G. ruber* appeared to live at depths of 0–50 m; the season of greatest abundance was summer to autumn. Generally, past summer and winter SSTs

Kim *et al. Progress in Earth and Planetary Science* (2015) 2:43

Page 15 of 16

can be reconstructed from planktonic foraminiferal assemblages. Alkenone- and Mg/Ca-based temperatures reconstructed from core-top sediments of the OT are consistent with observed (JODC dataset) annual mean SSTs and summer to autumn (June–November) SSTs, respectively. Core-top summer SSTs from planktonic foraminiferal assemblages represent observed August SSTs, whereas winter SSTs are approximately 3.6 °C warmer than observed February SSTs. During the late Holocene, 3-ky-averaged temperatures reconstructed from the various proxies were consistent with the current observed temperatures (JODC dataset) except for winter SSTs estimated using foraminiferal assemblages. These winter SSTs were higher than the current February SST. When the 3-ky-averaged temperatures during the late Holocene were compared with the SSTs during the LGM (Fig. 6), the foraminiferal assemblage-based August SSTs were warmest, and the alkenone- and Mg/Ca-based temperature estimates were similar to each other. However, the February foraminiferal assemblage-based SSTs were 2.7–3.7 °C cooler than the alkenone- and Mg/Ca-based temperature estimates during the late Holocene, although foraminiferal assemblage-based SSTs were consistent with other proxy temperatures during the LGM. The February foraminiferal assemblage-based SSTs were found to be greatly affected by the statistical technique and/or database used for calibration and estimation. Alkenone- and Mg/Ca ratio-based temperature estimates are not affected by the geochemical analytical method used for quantification or by the calibration equations chosen for calculations. Thus, alkenones and Mg/Ca appear to be the most robust choices for paleothermometry in the OT.

During the LGM, SSTs were 3 °C cooler than today, and SSSs were almost the same or 1 psu saltier, which might indicate that the summer East Asian monsoon had a weaker influence than it does today. It appears that the Kuroshio still influenced the area. The SST of the OT increased sharply with the onset of the late deglaciation between 16–15 cal ky BP. Relatively, saline surface water dominated over the middle OT during 16–12 cal ky BP, indicating that the strength of the Kuroshio increased at that time. The YD was identified in the northern and middle OT. Millennial-scale variations between warmer, more saline and cooler, less saline surface water during the deglaciation and the Holocene were identified from the core located in the northern OT, indicating changes in the mixing ratio between the Kuroshio water and the Changjiang diluted water. Comparisons of the hydrography records from the OT and the records of stalagmites in China, Tropical Pacific, and North Atlantic show that there is a teleconnection between the East Asian summer monsoon and the North Atlantic climate.

Abbreviations
AT: Aira-Tanzawa; GDGT: glycerol dibiphytanyl glycerol tetraether; IKM: Imbrie and Kipp transfer function method; JODC: Japan Oceanographic Data Center; K-Ah: Kikai-Akahoya; KC: Kuroshio Current; LGM: last glacial maximum; MAT: modern analog technique; OT: Okinawa Trough; PME: *Pulleniatina* Minimum Event; RAM: revised analog method; SSS: sea surface salinity; SST: sea surface temperature; YD: Younger Dryas climate event.

Competing interests
The authors declare that they have no competing interests.

Authors' contributions
RA prepared the manuscript and figures. KE designed and guided the preparation of manuscript and revised the manuscript. SW helped prepare the manuscript. All authors read and approved the final manuscript.

References
Anand P, Elderfield H, Conte MH. Calibration of Mg/Ca thermometry in planktonic foraminifera from a sediment trap time series. Paleoceanography. 2003;18(2):1050. doi:10.1029/2002PA000846.

Bé AWH, Tolderlund DS. Distribution and ecology of living planktonic foraminifera in surface waters of the Atlantic and Indian Oceans. In: Funnel BM, Riedel WR, editors. Micropaleontology of Oceans. London: Cambridge University Press; 1971. p. 105–49.

Bijma J, Faber Jr WW, Hemleben C. Temperature and salinity limits for growth and survival of some planktonic foraminifers in laboratory cultures. J Foram Res. 1990;20(2):95–116.

Boudreau BP. Is burial velocity a master parameter for bioturbation? Geochim Cosmochim Acta. 1994;58(4):1243–9.

Brassell SC, Eglinton G, Marlowe IT, Pflaumann U, Sarnthein M. Molecular stratigraphy: a new tool for climatic assessment. Nature. 1986;320:129–33.

Chang Y-P, Wang W-L, Yokoyama Y, Matsuzaki H, Kawahata H, Chen M-T. Millennial-scale planktic foraminifer faunal variability in the East China Sea during the past 40000 years (IMAGES MD012404 from the Okinawa Trough). Terr Atmos Ocean Sci. 2008;19(4):389–401. doi:10.3319/TAO.2008. 19.4.389(IMAGES).

Chang Y-P, Chen M-T, Yokoyama Y, Matsuzaki H, Thompson WG, Kao S-J, et al. Monsoon hydrography and productivity changes in the East China Sea during the past 100,000 years: Okinawa Trough evidence (MD012404). Paleoceanography. 2009;24:PA3208. doi:10.1029/2007PA001577.

Chen M-T, Huang C-C, Pflaumann U, Waelbroeck C, Kucera M. Estimating glacial western Pacific sea-surface temperature: methodological overview and data compilation of surface sediment planktic foraminifer faunas. Quat Sci Rev. 2005;24:1049–62.

Chen M-T, Lin XP, Chang Y-P, Chen Y-C, Lo L, Shen C-C, et al. Dynamic millennial-scale climate changes in the northwestern Pacific over the past 40,000 years. Geophys Res Lett. 2010;37:L23603. doi:10.1029/2010GL045202.

Dekens PS, Lea DW, Pak DK, Spero HJ (2002). Core top calibration of Mg/Ca in tropical foraminifera: refining paleotemperature estimation. Geochem Geophys Geosyst 3(4). doi:10.1029/2001GC000200

Elderfield H, Ganssen G. Past temperature and $\delta^{18}O$ of surface ocean waters inferred from foraminiferal Mg/Ca. Nature. 2000;405:442–5.

Hastings D, Kienast M, Steinke S, Whitko AA (2001) A comparison of three independent paleotemperature estimates from a high resolution record of deglacial SST records in the tropical South China Sea. Eos Trans AGU 82(47) Fall Meet Suppl Abstract PP12B-10

Horikawa K, Kodaira T, Zhang J, Murayama M. $\delta^{18}O_{sw}$ estimate for *Globigerinoides ruber* from core-top sediments in the East China Sea. 2015.

Ijiri A, Wang L, Oba T, Kawahata H, Huang C-Y, Huang C-Y. Paleoenvironmental changes in the northern area of the East China Sea during the past 42,000 years. Palaeogeogr Palaeoclimatol Palaeoecol. 2005;219:239–61. doi:10.1016/j.palaeo.2004.12.028.

Kim *et al. Progress in Earth and Planetary Science* (2015) 2:43

Page 16 of 16

Imbrie J, Kipp NG. A new micropaleontological method for quantitative paleoclimatology: application to a Late Pleistocene Caribbean core. In: Turekian KK, editor. The Late Cenozoic Glacial Ages. New Haven: Yale University Press; 1971. p. 71–181.

Jian Z, Wang P, Saito Y, Wang J, Pflaumann U, Oba T, et al. Holocene variability of the Kuroshio current in the Okinawa Trough, northwestern Pacific Ocean. Earth Planet Sci Lett. 2000;184:305–19.

Kao SJ, Wu C-R, Hsin YC, Dai M. Effects of sea level change on the upstream Kuroshio Current through the Okinawa Trough. Geophys Res Lett. 2006;33:L16604. doi:10.1029/2006GL026822.

Kao SJ, Dai MH, Wei KY, Blair NE, Lyons WB. Enhanced supply of fossil organic carbon to the Okinawa Trough since the last deglaciation. Paleoceanography. 2008;23:PA2207. doi:10.1029/2007PA001440.

Kubota Y, Kimoto K, Tada R, Oda H, Yokoyama Y, Matsuzaki H. Variations of East Asian summer monsoon since the last deglaciation based on Mg/Ca and oxygen isotope of planktic foraminifera in the northern East China Sea. Paleoceanography. 2010;25:PA4205. doi:10.1029/2009PA001891.

Lee KE, Schneider R. Alkenone production in the upper 200 m of the Pacific Ocean. Deep-Sea Res I. 2005;52:443–56. doi:10.1016/j.dsr.2004.11.006.

Lee KE, Lee HJ, Park J-H, Chang Y-P, Ikehara K, Itaki T, et al. Stability of the Kuroshio path with respect to glacial sea level lowering. Geophys Res Lett. 2013;40:392–6. doi:10.1012/GRL.50102.

Li T, Liu Z, Hall MA, Berne S, Saito Y, Cang S, et al. Heinrich event imprints in the Okinawa Trough: evidence from oxygen isotope and planktonic foraminifera. Palaeogeogr Palaeoclimatol Palaeoecol. 2001;176:133–46.

Lin H-L, Wang W-C, Hung G-W. Seasonal variation of planktonic foraminiferal isotopic composition from sediment traps in the South China Sea. Mar Micropaleontol. 2004;53:447–60. doi:10.1016/j.marmicro.2004.08.004.

Lin H-L. The seasonal succession of modern planktonic foraminifera: Sediment traps observations from southwest Taiwan waters. Cont Shelf Res. 2014;84:13–22. http://dx.doi.org/10.1016/j.csr.2014.04.020.

Lin Y-S, Wei K-Y, Lin I-T, Yu P-S, Chiang H-W, Chen C-Y, et al. The Holocene *Pulleniatina* Minimum Event revisited: Geochemical and faunal evidence from the Okinawa Trough and upper reaches of the Kuroshio current. Mar Micropaleontol. 2006;59:153–70. doi:10.1016/j.marmicro.2006.02.003.

Machida H. Volcanoes and tephras in the Japan area. Global Environ Res. 2002;6(2):19–28.

Müller PJ, Kirst G, Ruhland G, von Storch I, Rosell-Melé A. Calibration of the alkenone paleotemperature index U^{K}_{37} based on core-tops from the eastern South Atlantic and the global ocean (60°N-60°S). Geochim Cosmochim Acta. 1998;62(10):1757–72.

Nakanishi T, Yamamoto M, Tada R, Oda H. Centennial-scale winter monsoon variability in the northern East China Sea during the Holocene. J Quat Sci. 2012a;27(9):956–63. doi:10.1002/jqs.2589.

Nakanishi T, Yamamoto M, Irino T, Tada R. Distribution of glycerol dialkyl glycerol tetraethers, alkenones and polyunsaturated fatty acids in suspended particulate organic matter in the East China Sea. J Oceanogr. 2012b;68:959–70. doi:10.1007/s10872-012-0146-4.

Nürnberg D, Bijma J, Hemleben C. Assessing the reliability of magnesium in foraminiferal calcite as a proxy for water mass temperatures. Geochim Cosmochim Acta. 1996;60(5):803–14.

Ohkouchi N, Kawamura K, Kawahata H, Okada H. Depth ranges of alkenone production in the central Pacific Ocean. Global Biogeochem Cycles. 1999;13(2):695–704.

Ortiz JD, Mix AC. Comparison of Imbrie-Kipp transfer function and modern analog temperature estimates using sediment trap and core top foraminiferal faunas. Paleoceanography. 1997;12:175–90.

Pflaumann U, Duprat J, Pujol C, Labeyrie LD. SIMMAX: A modern analog technique to deduce Atlantic sea surface temperatures from planktonic foraminifera in deep-sea sediments. Paleoceanography. 1996;11(1):15–35.

Pflaumann U, Jian Z. Modern distribution patterns of planktonic foraminifera in the South China Sea and western Pacific: a new transfer technique to estimate regional sea-surface temperatures. Mar Geol. 1999;156:41–83.

Prahl FG, Muehlhausen LA, Zahnle DL. Further evaluation of long-chain alkenones as indicators of paleoceanographic conditions. Geochim Cosmochim Acta. 1988;52:2303–10.

Prell WL (1985) The stability of low-latitude sea-surface temperatures: An evaluation of the CLIMAP reconstruction with emphasis on the positive SST anomalies. United States Department of Energy, Office of Energy Research, TR025, vol. 1–2. Government Printing Office, US, pp 1–60

Rosell-Melé A, Bard E, Emeis K-C, Grimalt JO, Müller P, Schneider R, et al. Precision of the current methods to measure the alkenone proxy U^{K}_{37} and absolute alkenone abundance in sediments: Results of an interlaboratory comparison study. Geochem Geophys Geosyst. 2001;2:2000GC000141.

Rosenthal Y, Perron-Cashman S, Lear CH, Bard E, Barker S, Billups K, et al. Interlaboratory comparison study of Mg/Ca and Sr/Ca measurements in planktonic foraminifera for paleoceanographic research. Geochem Geophys Geosyst. 2004;5(4):Q04D09. doi:10.1029/2003GC000650.

Sawada K, Handa N, Nakatsuka T. Production and transport of long-chain alkenones and alkyl alkenoates in a sea water column in the northwestern Pacific off central Japan. Mar Chem. 1998;59:219–34.

Sun Y, Oppo DW, Xiang R, Liu W, Gao S. Last deglaciation in the Okinawa Trough: subtropical northwest Pacific link to northern hemisphere and tropical climate. Paleoceanography. 2005;20:PA4005. doi:10.1029/2004PA001061.

Tanaka Y. Coccolith fluxes and species assemblages at the shelf edge and in the Okinawa Trough of the East China Sea. Deep-Sea Res II. 2003;50:503–11.

Ternois Y, Sicre M-A, Boireau A, Marty J-C, Miquel J-C. Production pattern of alkenones in the Mediterranean Sea. Geophys Res Lett. 1996;23(22):3171–4.

Thompson PR. Planktonic foraminifera in the western north Pacific during the past 150 000 years: comparison of modern and fossil assemblages. Palaeogeogr Palaeoclimatol Palaeoecol. 1981;35:241–79.

Ujiié H, Hatakeyama Y, Gu XX, Yamamoto S, Ishiwatari R, Maeda L. Upward decrease of organic C/N ratios in the Okinawa Trough cores: proxy for tracing the post-glacial retreat of the continental shore line. Palaeogeogr Palaeoclimatol Palaeoecol. 2001;165:129–40.

Ujiié Y, Ujiié H, Taira A, Nakamura T, Oguri K. Spatial and temporal variability of surface water in the Kuroshio source region, Pacific Ocean, over the past 21,000 years: evidence from planktonic foraminifera. Mar Micropaleontol. 2003;49:335–64. doi:10.1016/S0377-8398(03)00062-8.

van Donk J. δ^{18}O as a tool for micropalaeontologists. In: Ramsay ATS, editor. Oceanic Micropalaeontology. London: Academic Press; 1977. p. 1345–70.

Waelbroeck C, Labeyrie L, Duplessy J-C, Guiot J, Labracherie M, Leclaire H, et al. Improving past sea surface temperature estimates based on planktonic fossil faunas. Paleoceanography. 1998;13(3):272–83.

Waelbroeck C, Labeyrie L, Michel E, Duplessy JC, McManus JF, Lambeck K, et al. Sea-level and deep water temperature changes derived from benthic foraminifera isotopic records. Quat Sci Rev. 2002;21:295–305.

Wang YJ, Cheng H, Edwards RL, An ZS, Wu YJ, Shen CC, et al. A high-resolution absolute-dated late Pleistocene monsoon record from Hulu cave, China. Science. 2001;294:2345–8.

Xu X, Oda M. Surface-water evolution of the eastern East China Sea during the last 36,000 years. Mar Geol. 1999;156:285–304.

Xu X, Yamasaki M, Oda M, Honda MC. Comparison of seasonal flux variations of planktonic foraminifera in sediment traps on both sides of the Ryukyu Islands, Japan. Mar Micropaleontol. 2005;58:45–55. doi:10.1016/j.marmicro. 2005.09.002.

Yamasaki M, Oda M. Sedimentation of planktonic foraminifera in the East China Sea: evidence from a sediment trap experiment. Mar Micropaleontol. 2003;49:3–20. doi:10.1016/S0377-8398(03)00024-0.

Yu H, Liu Z, Berne S, Jia G, Xiong Y, Dickens GR, et al. Variations in temperature and salinity of the surface water above the middle Okinawa Trough during the past 37 kyr. Palaeogeogr Palaeoclimatol Palaeoecol. 2009;281:154–64. doi:10.1016/j.palaeo.2009.08.002.

Yuan D, Cheng H, Edwards RL, Dykoski CA, Kelly MJ, Zhang M, et al. Timing, duration, and transitions of the last interglacial Asian monsoon. Science. 2004;304:575–8.

Zhou H, Li T, Jia G, Zhu Z, Chi B, Cao Q, et al. Sea surface temperature reconstruction for the middle Okinawa Trough during the last glacial– interglacial cycle using C_{37} unsaturated alkenones. Palaeogeogr Palaeoclimatol Palaeoecol. 2007;246:440–53. doi:10.1016/j.palaeo.2006.10.011.